HHS Public Access

Author manuscript

Prostate. Author manuscript; available in PMC 2018 February 16.

Published in final edited form as:

Prostate. 2016 October ; 76(14): 1312–1325. doi:10.1002/pros.23221.

Neuronal Trans-differentiation in Prostate Cancer Cells

Andrew Farach[1,*], **Yi Ding**[3,*], **MinJae Lee**[4], **Chad Creighton**[8], **Nikki A. Delk**[2], **Michael Ittmann**[6], **Brian Miles**[7], **David Rowley**[5], **Mary C. Farach-Carson**[2,5], and **Gustavo E. Ayala**[4]

[1]Department of Radiology, Division of Radiation Oncology, Baylor College of Medicine, Houston, TX

[2]Department of Biochemistry and Cell Biology, MS-140, Rice University, Houston, Texas

[3]Department of Pathology and Laboratory Medicine, University of Texas Health Science Center at Houston, Houston, TX

[4]Center for Clinical and Translational Sciences, University of Texas Health Science Center at Houston, Houston, TX

[5]Department of Molecular and Cell Biology, Baylor College of Medicine, Houston, TX

[6]Department of Pathology, Baylor College of Medicine, Houston, TX

[7]Department of Urology, Houston Methodist Hospital, Houston, TX

[8]Department of Medicine, Baylor College of Medicine, Houston, TX

Abstract

Neuroendocrine (NE) differentiation in prostate cancer (PCa) is an aggressive phenotype associated with therapy resistance. The complete phenotype of these cells is poorly understood. Clinical classification is based predominantly on the expression of standard NE markers. We analyzed the phenotype of NE carcinoma of the prostate utilizing *in vitro* methods, *in silico*, and immunohistochemical analyses of human disease.

Results—LNCaP cells, subjected to a variety of stressors (0.1% (v/v) fetal bovine serum, cyclic AMP) induced a reproducible phenotype consistent with neuronal trans-differentiation. Cells developed long cytoplasmic processes resembling neurons. As expected, serum deprived cells had decreased expression in androgen receptor and prostate specific antigen. A significant increase in neuronal markers also was observed. Gene array analysis demonstrated that LNCaP cells subjected to low serum or cAMP showed statistically significant manifestation of a human brain gene expression signature. In an *in silico* experiment using human data, we identified that only hormone resistant metastatic prostate cancer showed enrichment of the “brain profile”. Gene ontology analysis demonstrated categories involved in neuronal differentiation. Three neuronal markers were validated in a large human tissue cohort. This study proposes that the later stages of PCa

Corresponding Author: Gustavo E. Ayala, M.D.Department of Pathology and Laboratory Medicine, University of Texas Health Sciences Center Houston, School of Medicine, Houston, TX 77030, Tel: (713) 500 5356, Cell: (713) 444-9887, Gustavo.E.Ayala@uth.tmc.edu.

*Co-First Author

Conflict of Interest: The Authors have no conflicts to report that they believe could be construed as resulting in an actual, potential, or perceived conflict of interest with regard to the manuscript submitted for review.

evolution involves neuronal trans-differentiation, which would enable PCa cells to acquire independence from the neural axis, critical in primary tumors.

Keywords

prostate cancer; nerves; neurons; neuronal trans-differentiation; neuroendocrine; resistance phenotype; neuroendocrine; small cell

Introduction

Prostate cancer (PCa) cells rely principally on steroid hormones for growth and proliferation. The androgen receptor (AR) is nearly ubiquitously expressed in PCa cells. For this reason, androgen deprivation therapy (ADT) has been used as a means to slow progression of advanced disease and as adjuvant therapy for high-risk local disease. ADT is supported by decreased rates of spinal cord compression, ureteral obstruction, and extraskeletal metastasis in advanced disease (1, 2) as well as increased five year (3-5) and ten year (6) survival in high-risk local disease (2). Unfortunately, many of these patients will eventually develop metastatic castration resistant prostate cancer (mCRPC), with a median survival of fewer than two years despite aggressive chemotherapy (7).

Neuroendocrine (NE) carcinoma is most common in patients who have undergone ADT (8). It is apparent that clinical manipulations, predominantly ADT, select for this resistance to therapy phenotype over time, and favor androgen-independent disease progression (9-11) often leading to patient demise. New drugs that target the androgen axis more effectively have increased development of mCRPC.

Neuroendocrine differentiation (NED) in PCa classically is defined as the transformation of acinar PCa cells to an aggressive form of disease that expresses markers typical of NE cells. However, the definition of NED in PCa is rather general, encompassing a broad spectrum of disease phenotypes. On one side of the spectrum is prostatic small cell carcinoma (SCC), with clearly described morphologic features and NE markers assessed by immunohistochemistry. The most commonly used markers of NED in these cases are chromogranin A (ChrA) and synaptophysin. On the other side of the spectrum are morphologically defined acinar tumors that express NE markers to varying degrees. While the former is associated with adverse prognosis, the clinical significance of NE markers in the latter is unclear. For the purposes of this article, we will refer to NE carcinomas as those with the full phenotype of SCC in humans, or those that are associated with high risk of disease progression to lethality.

In vitro models for the NE phenotype have been developed. The most accepted model system involves the addition of cyclic AMP (cAMP) to LNCaP cells, and the NE classification is based on expression of ChrA and synaptophysin. Our group has shown that the addition of medium conditioned by bone marrow stromal cells or co-culture with bone marrow stromal cells induces NED in a subset of cells (12). Follow up studies demonstrated that factors in bone marrow, such as interleukin-6, can induce autophagy in PCa cells, a phenomenon that may be associated with the small cell phenotype (13). Additionally, transgenic mice have been created that spontaneously give rise to cells that mimic the NE

phenotype, such as the TRAMP model (14, 15). However, the true phenotype of these cells, described as having undergone NED, either *in vitro* or in human patient specimens, has not been well defined.

Our group also has proposed that nerves are paramount for cancer growth. Cancer cells induce new nerve growth (axonogenesis and neurogenesis) and this process starts at the pre-neoplastic stage. Higher nerve density is associated with more aggressive disease (16). Finally, the interaction between cancer and nerves in perineural invasion results in a symbiotic process wherein both the cancer and the nerves benefit (17). It is therefore plausible that nerves provide an alternate regulatory mechanism to hormonal regulation for the survival of PCa cells in the absence of androgen. If so, neuronal trans-differentiation would be necessary for the independence of cancer cells from their microenvironment and would permit a more aggressive growth.

It has been widely accepted that fully differentiated cells are committed and thus unable to significantly alter their phenotype. More recently, the concept of trans-differentiation, or the transition of a cell from one fully differentiated cell type to another completely distinguishable type, has been described through a process of cell plasticity (18). Importantly for the hypothesis of epithelial-neuronal trans-differentiation in PCa, a predictable and reproducible epithelial-neuronal transition has been described *in vivo* through a trans-differentiation event in *Caenorhabditis elegans* (19). This process may manifest clinically in humans as metaplasia.

In this article, we explored the nature of the neural phenotype of PCa, utilizing *in vitro* methods, *in silico*, and immunohistochemical analyses of human disease. These experiments were derived from morphologic observations of LNCaP cells under adverse conditions. Our results suggest that the stress phenotype goes beyond what has been traditionally described as NED. We present data demonstrating that these PCa cells and human SCC acquire a phenotype more accurately resembling neuronal trans-differentiation, than exclusively neuroendocrine changes.

Results

Morphological, phenotypic and growth rate changes in transdifferentiating LNCaP cells

We identified stark morphological changes in serum deprived LNCaP cells (0.1% (v/v) FBS), as well as those treated with cAMP when observed by light microscopy. Most cells developed many long cytoplasmic processes, with secondary and tertiary branching, well beyond 3 to 5 times the length of the cell body (Figure 1 A&B). These changes are not due to a retraction artifact, and have typically been assumed to be a manifestation of a NE phenotype. Because of the similarities with neuronal projections, we compared the morphological features of treated LNCaP cells to PC12 cells treated with nerve growth factor (NGF), a currently accepted model for neuronal cells, and observed striking similarities (Figure 1C-E compared to 1G-I). The morphologic changes in serum deprived (0.1% FBS) LNCaP cells were reversible with reintroduction of serum (Figure 1F). NGF (10 ng/ml) did not trigger large changes in morphology of LNCaP cells (Figure 1F).

To determine if observed morphological and growth changes were accompanied by changes in phenotype and cell function, we stained for normal prostate cell markers including prostate specific antigen (PSA) and androgen receptor (AR). Cells in complete serum expressed AR largely in the nucleus (compare green signal to nuclear marker DAPI; Figure 1J). Serum deprived cells (0.1% FBS) had decreased levels of AR (Figure 1J). Cells in complete medium expressed robust levels of PSA, with the majority appearing extranuclear (compare green signal to DAPI, Figure 1K). Reduction of FBS reduced overall signal for PSA, including that in cellular processes (arrow).

Next, classical NED marker expression was assessed by ChrA staining. Cells in complete medium expressed low levels of ChrA, which appeared to be in the secretory pathway. Reduction in serum dramatically upregulated levels of ChrA protein, which were distributed throughout the processes (arrows) (Figure 2A). To explore if the projections were a manifestation of neuronal trans-differentiation, we tested also for neuronal markers within the cells. Neurofilament-M (NF-M) was diffusely expressed in cells growing in 10% FBS, with increased expression in cells growing in reduced serum (Figure 2B). Expression of NF-M could be seen extending all the way down processes to the tips (arrowhead).

To confirm the neuronal nature of the transdifferentiated cells, a panel of markers was used in immunostaining. Neuronal markers tested included neuron specific enolase (NSE) (Figure 2C), S-100 (Figure 2D), neuronal nuclei (NeuN) (Figure 2E), and beta tubulin III (Figure 2F). Staining for all four of these markers was much more intense in cells treated with 0.1% FBS compared to 10% FBS controls. Additionally, all four markers were expressed along neurite-looking extensions and within the cell body. This allowed reliable visualization of cell processes that could not be seen with DAPI.

In silico studies of human tissue PCa specimens

To extend our *in vitro* observations to a human gene expression context, we analyzed public databases containing archived gene expression data for brain and non-brain tissue (see methods). Of 4447 genes examined, we found 2302 genes that are expressed in normal brain tissues at higher levels than in other normal epithelial tissues (Figure 3C left). This data was used to establish a signature that we call the “brain profile”.

The pattern of gene expression in LNCaP cells treated with 0.1% FBS, cAMP, semaphorin 4F (S4F) or apoptosis-stimulating of p53 protein 2 (ASPP2) (and controls) that had undergone trans-differentiation were compared to the original brain profile. These comparisons revealed statistically significant enrichment of serum deprived cells and cAMP signatures within the human brain signature (Figure 3A). In contrast, cells transfected with ASPP2 or S4F did not show the common patterns consistent with their lack of morphological features resembling neurons.

We compared the “brain profile” to gene array patterns associated with prostate epithelial cells and PCa at different stages including localized, metastatic and hormone resistant cancer (MET-HR). We identified enrichment of the “brain profile” genes only on the MET-HR set. In the MET-HR specimen microarray, 988 genes were upregulated in MET-HR over treatment responsive PCa controls (Figure 3 B&C). The upregulated genes common to both

the “brain profile” and the MET-HR profile was significant (p<1e-07), with 274 of 988 upregulated genes in MET-HR (28%) overlapping with the brain signature (Figure 3B). The same process was performed to determine genes with decreased expression in both MET-HR and the brain signature. In this case, 163 genes were down regulated in both groups but were not statistically significant (data not shown).

After identifying the 274 common genes with increased expression in both brain and MET-HR, and the 163 common genes with decreased expression in these same datasets, *in silico* studies were performed using a gene ontology (GO) database (WebGestalt) to identify the primary biological processes, molecular functions, and cellular components of gene products common to brain and MET-HR (Tables 1 and 2). Only the top ten most significant biological processes, molecular functions, and cellular components are listed for both up regulated (Table 1) and down regulated genes (Table 2). It is immediately clear from an examination of gene function data that many of the changes in gene expression in MET-HR are consistent with morphological changes observed in neuronal differentiation and axonogenesis. For example in examining the group of biological processes, 54 (~20%) of the 274 genes are associated with development of the nervous system, 8% are associated with synaptic transmission, and 6.6% are associated with neuron differentiation or neuron projections. These functions are not related to endocrine secretion, but rather neuronal structural elements that distinguish them from NE cells. Likewise, down-regulated processes reflect dynamic changes in cellular homeostasis, organization and cell function.

Examination of genes associated with molecular functions suggests large changes in cellular complexes in HR-MET over treatment responsive PCa. Fully 60% of the upregulated gene products have an association with protein binding, indicative of changing cellular machinery. Many, 27 of 274 (10 %), have kinase activity. Interestingly, a majority (63%) of proteins highly expressed in MET-HR, and common to brain, are predicted to be found in the cytosol, when analyzed for cellular components. Those down-regulated genes include a number associated with microtubules or centrosomes. A significant loss of cytoplasm and cytoplasmic part genes (62% and 40%, respectively) also is seen, consistent with a small cell phenotype of MET-HR.

Finally, the genes most highly enriched in the brain in MET-HR do not overlap with the FBS or cAMP signatures, although some were common (data not shown). It is clear that the MET-HR signature and the LNCaP transdifferentiated signatures are distinct, although both are highly consonant with the brain signature. This is likely a manifestation of *in vitro* growth conditions in contrast to human biological conditions.

Validation of Neuronal markers in human tissues

We selected three antibodies from the 274 upregulated genes in MET-HR overlapping with the “brain profile”. These antibodies were chosen from categories that would help demonstrate neuronal differentiation and had commercially available antibodies. The distinction of a neuroendocrine cell and a neuron is best achieved by analyzing the distal end of the cell. Hence we choose axonal, synaptic and ion channel proteins from the list of up-regulated genes. Neurons have voltage-gated ion channels embedded in a cell's plasma membrane that are in charge of creating membrane potential. We selected a sodium channel,

the voltage-gated, type III, beta (SCN3B). Neurons have distal axons. We choose an axonal related protein, contactin associated protein 1 (CNTNAP1). This protein may be the signaling subunit of contactin, enabling recruitment and activation of intracellular signaling pathways in neurons. Contactin may play a role in the formation of axon connections in the developing nervous system. The distal machinery to release neurotransmitters (active zone) is composed of synaptic vesicles and a meshwork of cytoskeleton. Bassoon presynaptic cytomatrix protein (BSN) is thought to be a scaffolding protein involved in organizing the presynaptic cytoskeleton and is expressed primarily in neurons in the brain.

We found very weak and very focal expression of contactin associated protein 1 (CNTNAP1), and sodium channel, voltage-gated, type III, beta (SCN3B) in primary prostate tumors. Levels of expression for both markers did not significantly change in metastatic hormone naive prostate cancer (MET-HN). However, we found increased levels of expression, and usually diffuse expression, in prostatic SCC, for both SCN3B ($p=<0.0001$) and CNTNAP1 ($p=0.0014$), when compared to primary PCa; or to MET-HN; SCN3B ($p=<0.0001$) and CNTNAP1 ($p=<0.0001$) (Figure 4A and 4B). Both CNTNAP1 and SCN3B showed cytoplasmic microgranular staining (Figures 4C and 4D). Another neuronal marker, bassoon presynaptic cytomatrix protein (BSN), was extensively present throughout prostatic SCC. The stain was mostly cytoplasmic and microgranular, but could be found as membranous/cytoplasmic dense punctate or linear staining possibly mimicking abortive synaptic structures (Figure 4E). Further, Spearmen correlation coefficient testing was performed using CNTNAP1, SCN3B, BSN, and Ki-67, in conjunction with several nuclear and cytoplasmic clinicopathological markers in intact prostate and MET-HN human PCa specimen. Analysis found high immunohistochemical correlation of neuronal calcium channel marker SCN3B with AR in MET-HN samples. CNTNAP1 only correlated with serine/threonine-protein kinase, Pim-2 ($r = 0.196$, $p = 0.056$) (Figure 5).

Discussion

The data presented in this study adds to the currently accepted paradigm of NED in PCa. Based on our results, we propose that MET-HR cells undergo a process of trans-differentiation in response to stress, representing a phenotype beyond NED with demonstrable attributes of a neuronal phenotype. This would be the consequence of the natural evolution of neural dependent cancer searching for independence for the neural axis.

The current definition of prostatic SCC relies heavily on the presence of ultrastructural dense core granules, and immunohistochemical stains, such as ChrA, to detect them. ChrA is a structural protein found in dense core granules, and indicates only the presence of the granule and not the products stored inside (peptides, amines or neurotransmitters). These neurosecretory granules can be found in multiple cell types, including NE cells, endocrine, exocrine, and hematopoietic cells. They can also be found in neurons (20) (21). Our study confirms the presence of neurosecretory granules in SCC of the prostate, but presents additional new findings indicating that the transdifferenratiaion goes beyond neuroendocrine into neuronal.

Our results are consistent with several previous studies, demonstrating NE trans-differentiation of LNCaP cells under various growth conditions. Many published studies describe morphologic changes with extension of large, branching axonal processes. This response is a well-accepted model for NED(22). While the list is too exhaustive to describe fully here, a few points are worth noting. NED-like differentiation is inducible with ADT (23-26), db-cAMP (27), IL-6 (13) (28), hormone depleted medium (25), transfection with constitutively active subunit of gp130 (29), protocadherin-pc (30), or ASPP2. In addition, treatment with melatonin (31) or co-culture of LNCaP cells with bone marrow stromal cells (12) induces similar phenotypic changes.

When comparing micrographs in these studies, it is evident that this phenotypic change is remarkably preserved and reproducible regardless of the pathway utilized for inducing NED. A plausible assumption from this observation is that the “brain profile”, as described, would be similarly up regulated under any NED inducing condition that produces this morphological feature. This finding indicates that PCa cells may have an encoded mechanism for neuronal trans-differentiation in response to various stress conditions as a means for survival.

In this study, we confirmed the enrichment of genes identified in a human brain signature in both MET-HR and transdifferentiating LNCaP cells. Within this overlapping profile, GO studies demonstrated that the most significantly upregulated biological processes encompass nervous system development and neuronal morphogenesis. Validation at the protein level showed positivity of several neuronal markers including NF-M, S100, NSE, β-tubulin, and NeuN in the transdifferentiating LNCaP model and SCN3B, CNTNAP1, and BSN in human prostate SCC. These data indicate that this process is more accurately described as neuronal trans-differentiation, as we identify neuronal developmental transcripts that are not “endocrine” functionally, gene products that are not secreted peptide ligands with cognate receptors.

Another major difference between a neuron and NE cell is the ability to transmit an action potential. Numerous publications have demonstrated that pulmonary SCC express voltage-dependent calcium, potassium and sodium channels and that the cancer cells can transmit action potential (32-34) (35) (36). Voltage-sensitive ion channels are increasingly thought to increase malignant potential through increased cell proliferation, migration and survival (37). Presynaptic proteins also have been described previously in pulmonary SCC (38).

We observed very weak and very focal expression of CNTNAP1 and SCN3B in primary prostate tumors. However we observed moderate to intense and diffuse staining of CNTNAP1 and SCN3B, as well as BSN, in all tested cases of prostatic SCC (n=7). Importantly, SCN3B expression correlated with AR expression in MET-HN without small cell differentiation, possibly indicating upregulation of voltage-dependent on channels and early invocation of the neuronal phenotype in metastatic hormone sensitive disease. The association of Pim-2 and CNTNAP1 was interesting in that we have previously shown an association between upregulated nuclear Pim-2 and both enhanced perineural invasion and PCa disease progression (39).

Understanding the role of nerves in primary tumors is paramount to understanding the rationale behind neuronal trans-differentiation of PCa cells. We have previously described cancer related neurogenesis and axonogenesis as a novel biologic phenomenon in PCa (17). This phenomenon was associated with aggressive human PCa and may lead to perineural invasion. The perineural space provides a survival advantage, where cancer cells show increased proliferation and decreased apoptosis (16) (40). Nerves regulate not only cancer, but also normal prostatic epithelium. Prostatic atrophy has been described in response to botulism neurotoxins and has been proposed as a potential mechanism for the treatment of benign prostatic hypertrophy (41). Our findings indicate that nerves play a role in the normal epithelial tissues homeostasis and are involved in PCa tumor survival (data not presented). Hence, while the primary regulatory axis for the prostate in adults is hormonal, the neural regulatory axis is probably the second most important growth regulatory axis in the prostate.

After acquiring the ability to metastasize through epithelial mesenchymal transformation, PCa cells establish metastatic foci. These are still under the regulatory control of blood borne hormones. During ADT the metastatic cancer cells, in the absence of the ligand effect, acquire features that permit growth independence form hormones. In a microenvironment unfavorable to neural recruitment, such as the bone marrow, and in the presence of bone marrow stromal cells, it is plausible that PCa cells would acquire independence from the neuronal axis. Hence, neuronal trans-differentiation becomes an escape mechanism that provides metastatic cancer cells ultimate growth independence. This phenomenon makes the cancer cells independent from all regulatory mechanisms, and permits the blast growth phase of PCa. The later growth phase characterizes this disease clinically.

Our proposed terminology for this phenotype is based on a sensible biological rationale; neuronal trans-differentiation, would provide independence from the neural axis, a critical axis in primary tumors. We do not claim that these PCa cells convert to fully functional neurons; rather they acquire neuronal features that may potentiate independence from the neural axis. Clearly, further studies are necessary to substantiate this conclusion. However, it opens the possibility of utilizing neurotoxins as a novel treatment approach to inhibit not only neuroepithelial interactions, but also deter the cell survival advantage conferred by neuronal trans-differentiation.

Materials and Methods

Cell Culture and Trans-differentiation

LNCaP cells were cultured in RPMI-1640 (Mediateck, Manassas, VA) containing 10% (v/v) fetal bovine serum (FBS) and 1% (v/v) penicillin/streptomycin. Cells were incubated at 37°C in a 5% CO_2 atmosphere in six-well plates. Various methods were used to induce a transdifferentiated phenotype similar to resistant cells *in vivo*:

a. cells were plated at 80,000 cells/well and grown to 30-50% confluence, then at 24 h were withdrawn to 0.1% (v/v) FBS for 12 days with medium changes every 2-3 days;

b. cells were plated at 80,000 cells/well and grown to 30-50% confluence, then at 24 h, cultured in cAMP as described in Bang *et al* (27); briefly, dibutyryl-cAMP

(db-cAMP) (Sigma-Aldrich, St. Louis, MO) and isobutylmethylxanthine (IBMX) (Sigma-Aldrich) at a concentration of 1 mM db-cAMP / 500 mM IBMX in 10% FBS. The medium was changed every two days. Cells were digitally photographed at day five.

c. ASPP2 expression plasmid pcDNA3.1-ASPP2, was a kind gift from Dr. Xin Lu (Ludwig Institute for Cancer Research, London, UK). LNCaP cells grown to 60% confluence in 10% FBS were transfected with 2 μg pcDNA3.1-ASPP2 or empty vector, plus 0.2 μg of plasmid DNA (pEGFP-C1) that codes for enhanced green fluorescence protein in duplicate. Two days later, transfection was confirmed by western blot. On days 5 and 7, >100 GFP-positive cells were counted for neuron-like cells in another well, based on morphologic changes, including the development of axonal projections.

d. LNCaP cells grown to 30-50% confluence in a T25 flask in RPMI-1640 and 10% FBS were transfected with S4F as described in Ayala *et al.* (17). Briefly, at 24 h, cell growth medium was removed and 1:1 mL/mL viral supernatant and 10% FBS containing 8 μg/mL polybrene was added to cells. Three hours later, cells were washed with PBS, and 5 mL fresh medium was added to cells. After 48 h, cells were separated and S4F expression was confirmed by western blot.

e. PC12 cells were grown under standardized conditions, including neural growth factor induction.

Proliferation assay

To determine cell growth and dynamics, LNCaP cells were plated into 6-well plates at a density of 80,000 cells/ well. Two days later, cells were washed with PBS, and fresh 10% or 0.1% FBS-RPMI 1640 medium was added to cells (Day 0). Viable cell number was determined at day 0, 3, 5, and 7 by Trypan-blue exclusion test and manual counting of viable cells.

Immunofluorescence

At day 5 of culture conditions, LNCaP cells were fixed with 4% (v/v) paraformaldehyde and permeabilized with 0.2% (v/v) Triton-X100. Cells were incubated with primary antibody for 1 h at room temperature (RT), then with FITC-coupled secondary antibody for 40 min at RT. Primary antibodies include: NF-M (NeoMarkers, Fremont, CA); NSE (NeoMarkers); S-100 (Dako, Carpinteria, CA); AR (BD Biosciences, San Jose, CA); PSA (NeoMarkers); ChrA (Vector Laboratories, Burlingame, CA); NeuN (Chemicon, Billerica, MA); and beta tubulin III (Chemicon).

RNA extraction and cDNA microarray

LNCaP cells were plated into 60 or 100 mm plates in 10% FBS. The next day, medium was replaced with fresh 10% or 0.1% FBS-RPMI 1640; treated with or without 1 mM db-cAMP/ 500 mM IBMX; transfected with pcDNA3.1-ASPP2 or empty vector (5μg/ well by FuGENE® HD Transfection Reagent; Promega, Madison, WI); infected with S4F or vector retrovirus (RV) as described above. Total RNA was extracted on day 6 (serum starvation),

day 5 (c-AMP treatment or S4F RV infection) and day 2 (ASPP2 transfection) by RNeasy Mini Kit (QIAGEN, Valencia, CA). The cDNA reverse transcription and fluorescent labeling reactions were carried out using SuperScript Plus Direct cDNA Labeling System with Alexa Fluor aha-dUTPs (Invitrogen, Carlsbad, CA). Briefly 2.5 mg of total RNA and Universal Human Reference RNA (Stratagene, La Jolla, CA) were labeled in reverse transcription with Alexa647 and Alexa555 aha-dUTPs, respectively. After labeling, each sample cDNA was mixed with an equal amount of labeled reference cDNA and purified with SuperScript™ Plus Direct cDNA Labeling System (Invitrogen, Grand Island, NY) purification module according to the manufacturer's instructions. Eluted sample was mixed with 10X blocking solution and 2X HiRPM buffer (Agilent Technologies, Palo Alto, CA) diluted up to 100 μl of volume, then incubated for 2 min at 95-98^{o} C. Aliquots (95 μl) then were loaded onto the slide, and hybridized on Agilent Whole Human Genome Oligo Microarrays 4x44K (Agilent Technologies, Santa Clara, CA) using SureHyb DNA Microarray Hybridization Chambers in DNA Microarray hybridization oven (Agilent) agitated at 10 rpm, 65^{o}C for 20 h. After hybridization, slides were washed in Gene Expression Wash Buffer that was pre-warmed at 37 °C for 1 min and then dried by centrifugation at 2000 rpm for 2 min. Microarrays were scanned with a dynamic autofocus microarray scanner (Agilent) using Agilent-provided parameters (Red and Green PMT were each set at 100%, and scan resolution was set to 5 μm). The Feature Extraction Software v9.1.3.1 (Agilent) was used to extract and analyze the signals.

In silico Analysis

Publically available gene expression databases of normal brain (Novartis Gene Atlas) versus epithelial tissues were interrogated via microarray to obtain a representative molecular signature: “brain profile”. There were 2302 unique named genes up in brain and 2237 unique named genes down. The resulting neuronal PCa profile was queried against gene expression profiles from LNCaP cells transdifferentiated under various conditions to determine which cells manifest a neuronal signature. Gene array profile datasets from the various experimental groups included 0.1% fetal bovine serum, cyclic AMP, ASPP and S4F (overexpression and empty vector controls) and appropriate controls. For each profiled sample, we derived a correlation value in relation to the brain signature. The correlation value was defined as the Pearson's correlation between the brain gene signature pattern (using “1” and “-1”, for up and down, respectively) and the sample's expression values.

In the next step, the “brain profile” was compared against publically available profiles of normal prostatic epithelial tissues, normal epithelia adjacent to cancer, pre-neoplastic high grade prostatic intraepithelial neoplasia, confined PCa, MET-HN, and MET-HR. Genes were identified whose expression was “up in brain” or “down in brain” when compared to epithelial tissues. A 2-fold expression change was used in these assignments. Next, genes expressed in MET-HR were compared to genes expressed in primary PCa specimens to select an “up in MET-HR” dataset. Finally, the “up in brain” profile was compared to the “up in MET-HR” profile to identify a common “neuronal prostate cancer” signature. A p-value of $p<0.01$ was used for the intersection of genes in the brain set with the genes higher in MET-HR vs. PCa.

Gene ontology trees then were constructed using WebGestalt (42) with a p-value set at 0.05 to identify biological processes, molecular function, and cellular components that appeared to be upregulated under various experimental conditions.

Validation in Human Tissues

For this study we used a tissue microarray from Baylor College of Medicine that contained tissues from primary tumors as well as metastatic tumor (2 mm cores). Initially, the tissue microarray contained tissues from 36 primary tumors and 174 metastases (9 bone, 1 brain, 1 liver, 1 lung, 1 paraspinal, 1 spinal cord, 1 thymus and 159 lymph nodes). Due to previous utilization of the array and variable thickness of tissues derived from multiple sources, data is available in a variable and lower number of cases. Seven cases of prostatic SCC also were used.

Immunohistochemistry

We selected commercially available antibodies based on functions associated with neuronal rather than NE functions. Antibodies CNTNAP1 (contactin associated protein 1), Basson (presynaptic cytomatrix protein) and SCN3B (Sodium Chanel, voltage-gated, type III, beta) were purchased from Sigma Aldrich (cat. # HPA011772, HPA034757 and HPA042518, respectively).

Slides were deparaffinized in xylene and graded alcohol. Heat induced antigen retrieval was carried out by pressurized heating in the Pascal pressure chamber (Dako), in Citrate buffer (pH 6.0), for 10 min at 125 °C (CNTNAP1) or for 4 min at 125 °C (BSN and SCN3B). Endogenous peroxidase activity was blocked using 3% H2O2 for 10 min.

Antibodies to CNTNAP1 (1:50 dilution), and BSN (1:150 dilution) were incubated at 4 °C overnight, while that to SCN3B (1:100 dilution) were incubated at RT for 1h. The VECTASTAIN Elite ABC kit (Vector Laboratories) was applied for CNTNAP1 and MACH 4™ Universal HRP-Polymer (Biocare Concord, CA) was applied for BSN and SCN3B. Slides were counterstained with CAT hematoxylin (Biocare) and mounted in CYTOSEAL XYL (ThermoFisher Scientific, Waltham, MA). A semiquantitaive method from 0-3 was used, with 0 being no expression, 1 low expression in scattered cells, 2 medium expression in less than 50% of cells, and 3 strong and diffuse expression.

Statistical Analysis

Correlation of immunohistochemical localization with several clinicopathological markers was evaluated using Spearman correlation coefficient testing.

Acknowledgments

Support: This work was supported by National Institutes of Health (NIH) grant TMEN U54CA126568-01 (Ayala), a Prostate Cancer Foundation Creativity Award (Ayala), and NIH CA128296 (Delk) and NIH/NCI P01 CA098912 (Farach-Carson).

References

1. Immediate versus deferred treatment for advanced prostatic cancer: initial results of the Medical Research Council Trial. The Medical Research Council Prostate Cancer Working Party Investigators Group. Br J Urol. 1997; 79(2):235–46. Epub 1997/02/01. [PubMed: 9052476]
2. Sharifi N, Gulley JL, Dahut WL. Androgen deprivation therapy for prostate cancer. JAMA. 2005; 294(2):238–44. Epub 2005/07/15. DOI: 10.1001/jama.294.2.238 [PubMed: 16014598]
3. Bolla M, Collette L, Blank L, Warde P, Dubois JB, Mirimanoff RO, Storme G, Bernier J, Kuten A, Sternberg C, Mattelaer J, Lopez Torecilla J, Pfeffer JR, Lino Cutajar C, Zurlo A, Pierart M. Long-term results with immediate androgen suppression and external irradiation in patients with locally advanced prostate cancer (an EORTC study): a phase III randomised trial. Lancet. 2002; 360(9327): 103–6. Epub 2002/07/20. [PubMed: 12126818]
4. Bolla M, Gonzalez D, Warde P, Dubois JB, Mirimanoff RO, Storme G, Bernier J, Kuten A, Sternberg C, Gil T, Collette L, Pierart M. Improved survival in patients with locally advanced prostate cancer treated with radiotherapy and goserelin. N Engl J Med. 1997; 337(5):295–300. Epub 1997/07/31. DOI: 10.1056/nejm199707313370502 [PubMed: 9233866]
5. D'Amico AV, Manola J, Loffredo M, Renshaw AA, DellaCroce A, Kantoff PW. 6-month androgen suppression plus radiation therapy vs radiation therapy alone for patients with clinically localized prostate cancer: a randomized controlled trial. JAMA. 2004; 292(7):821–7. Epub 2004/08/19. DOI: 10.1001/jama.292.7.821 [PubMed: 15315996]
6. Messing EM, Manola J, Sarosdy M, Wilding G, Crawford ED, Trump D. Immediate hormonal therapy compared with observation after radical prostatectomy and pelvic lymphadenectomy in men with node-positive prostate cancer. N Engl J Med. 1999; 341(24):1781–8. Epub 1999/12/10. DOI: 10.1056/nejm199912093412401 [PubMed: 10588962]
7. Bracarda S, Logothetis C, Sternberg CN, Oudard S. Current and emerging treatment modalities for metastatic castration-resistant prostate cancer. BJU Int. 2011; 107(Suppl 2):13–20. Epub 2011/03/16. DOI: 10.1111/j.1464-410X.2010.10036.x [PubMed: 21382150]
8. Hirano D, Okada Y, Minei S, Takimoto Y, Nemoto N. Neuroendocrine differentiation in hormone refractory prostate cancer following androgen deprivation therapy. Eur Urol. 2004; 45(5):586–92. discussion 92. [PubMed: 15082200]
9. Rau KM, Kang HY, Cha TL, Miller SA, Hung MC. The mechanisms and managements of hormone-therapy resistance in breast and prostate cancers. Endocr Relat Cancer. 2005; 12(3):511–32. Epub 2005/09/21. DOI: 10.1677/erc.1.01026 [PubMed: 16172190]
10. Thompson IM, Goodman PJ, Tangen CM, Lucia MS, Miller GJ, Ford LG, Lieber MM, Cespedes RD, Atkins JN, Lippman SM, Carlin SM, Ryan A, Szczepanek CM, Crowley JJ, Coltman CA Jr. The influence of finasteride on the development of prostate cancer. N Engl J Med. 2003; 349(3): 215–24. Epub 2003/06/26. DOI: 10.1056/NEJMoa030660 [PubMed: 12824459]
11. Evangelou AI, Winter SF, Huss WJ, Bok RA, Greenberg NM. Steroid hormones, polypeptide growth factors, hormone refractory prostate cancer, and the neuroendocrine phenotype. J Cell Biochem. 2004; 91(4):671–83. Epub 2004/03/03. DOI: 10.1002/jcb.10771 [PubMed: 14991759]
12. Zhang C, Soori M, Miles FL, Sikes RA, Carson DD, Chung LW, Farach-Carson MC. Paracrine factors produced by bone marrow stromal cells induce apoptosis and neuroendocrine differentiation in prostate cancer cells. Prostate. 2011; 71(2):157–67. Epub 2010/07/29. DOI: 10.1002/pros.21231 [PubMed: 20665531]
13. Delk NA, Farach-Carson MC. Interleukin-6: A bone marrow stromal cell paracrine signal that induces neuroendocrine differentiation and modulates autophagy in bone metastatic PCa cells. Autophagy. 2012; 8(4) Epub 2012/03/24.
14. Tang Y, Wang L, Goloubeva O, Khan MA, Lee D, Hussain A. The relationship of neuroendocrine carcinomas to anti-tumor therapies in TRAMP mice. Prostate. 2009; 69(16):1763–73. Epub 2009/08/20. DOI: 10.1002/pros.21026 [PubMed: 19691128]
15. Huss WJ, Gray DR, Tavakoli K, Marmillion ME, Durham LE, Johnson MA, Greenberg NM, Smith GJ. Origin of androgen-insensitive poorly differentiated tumors in the transgenic adenocarcinoma of mouse prostate model. Neoplasia. 2007; 9(11):938–50. Epub 2007/11/22. [PubMed: 18030362]

16. Ayala GE, Dai H, Ittmann M, Li R, Powell M, Frolov A, Wheeler TM, Thompson TC, Rowley D. Growth and survival mechanisms associated with perineural invasion in prostate cancer. Cancer Res. 2004; 64(17):6082–90. Epub 2004/09/03. DOI: 10.1158/0008-5472.can-04-0838 [PubMed: 15342391]
17. Ayala GE, Dai H, Powell M, Li R, Ding Y, Wheeler TM, Shine D, Kadmon D, Thompson T, Miles BJ, Ittmann MM, Rowley D. Cancer-related axonogenesis and neurogenesis in prostate cancer. Clin Cancer Res. 2008; 14(23):7593–603. [PubMed: 19047084]
18. Tosh D, Slack JM. How cells change their phenotype. Nat Rev Mol Cell Biol. 2002; 3(3):187–94. Epub 2002/05/08. DOI: 10.1038/nrm761 [PubMed: 11994739]
19. Jarriault S, Schwab Y, Greenwald I. A Caenorhabditis elegans model for epithelial-neuronal transdifferentiation. Proc Natl Acad Sci U S A. 2008; 105(10):3790–5. Epub 2008/03/01. DOI: 10.1073/pnas.0712159105 [PubMed: 18308937]
20. Kloukina-Pantazidou I, Chrysanthou-Piterou M, Havaki S, Issidorides MR. Chromogranin A and vesicular monoamine transporter 2 immunolocalization in protein bodies of human locus coeruleus neurons. Ultrastruct Pathol. 2013; 37(2):102–9. Epub 2013/04/12. DOI: 10.3109/01913123.2012.750410 [PubMed: 23573890]
21. Bauer R, Ischia R, Marksteiner J, Kapeller I, Fischer-Colbrie R. Localization of neuroendocrine secretory protein 55 messenger RNA in the rat brain. Neuroscience. 1999; 91(2):685–94. Epub 1999/06/12. doi:S0306-4522(98)00668-X[pii]. [PubMed: 10366025]
22. Horoszewicz JS, Leong SS, Kawinski E, Karr JP, Rosenthal H, Chu TM, Mirand EA, Murphy GP. LNCaP model of human prostatic carcinoma. Cancer Res. 1983; 43(4):1809–18. Epub 1983/04/01. [PubMed: 6831420]
23. Burchardt T, Burchardt M, Chen MW, Cao Y, de la Taille A, Shabsigh A, Hayek O, Dorai T, Buttyan R. Transdifferentiation of prostate cancer cells to a neuroendocrine cell phenotype in vitro and in vivo. J Urol. 1999; 162(5):1800–5. Epub 1999/10/19. [PubMed: 10524938]
24. Jimenez N, Hernandez-Cruz A. Modifications of intracellular Ca2+ signalling during nerve growth factor-induced neuronal differentiation of rat adrenal chromaffin cells. Eur J Neurosci. 2001; 13(8):1487–500. Epub 2001/05/01. [PubMed: 11328344]
25. Shen R, Dorai T, Szaboles M, Katz AE, Olsson CA, Buttyan R. Transdifferentiation of cultured human prostate cancer cells to a neuroendocrine cell phenotype in a hormone-depleted medium. Urol Oncol. 1997; 3(2):67–75. Epub 1997/03/01. [PubMed: 21227062]
26. Yuan S, Rosenberg L, Paraskevas S, Agapitos D, Duguid WP. Transdifferentiation of human islets to pancreatic ductal cells in collagen matrix culture. Differentiation. 1996; 61(1):67–75. Epub 1996/10/01. DOI: 10.1046/j.1432-0436.1996.6110067.x [PubMed: 8921586]
27. Bang YJ, Pirnia F, Fang WG, Kang WK, Sartor O, Whitesell L, Ha MJ, Tsokos M, Sheahan MD, Nguyen P, Niklinski WT, Myers CE, Trepel JB. Terminal neuroendocrine differentiation of human prostate carcinoma cells in response to increased intracellular cyclic AMP. Proc Natl Acad Sci U S A. 1994; 91(12):5330–4. Epub 1994/06/07. [PubMed: 8202489]
28. Deeble PD, Murphy DJ, Parsons SJ, Cox ME. Interleukin-6- and cyclic AMP-mediated signaling potentiates neuroendocrine differentiation of LNCaP prostate tumor cells. Mol Cell Biol. 2001; 21(24):8471–82. Epub 2001/11/20. DOI: 10.1128/mcb.21.24.8471-8482.2001 [PubMed: 11713282]
29. Palmer J, Ernst M, Hammacher A, Hertzog PJ. Constitutive activation of gp130 leads to neuroendocrine differentiation in vitro and in vivo. Prostate. 2005; 62(3):282–9. Epub 2004/09/25. DOI: 10.1002/pros.20143 [PubMed: 15389784]
30. Yang X, Chen MW, Terry S, Vacherot F, Chopin DK, Bemis DL, Kitajewski J, Benson MC, Guo Y, Buttyan R. A human- and male-specific protocadherin that acts through the wnt signaling pathway to induce neuroendocrine transdifferentiation of prostate cancer cells. Cancer Res. 2005; 65(12): 5263–71. Epub 2005/06/17. DOI: 10.1158/0008-5472.can-05-0162 [PubMed: 15958572]
31. Sainz RM, Mayo JC, Tan DX, Leon J, Manchester L, Reiter RJ. Melatonin reduces prostate cancer cell growth leading to neuroendocrine differentiation via a receptor and PKA independent mechanism. Prostate. 2005; 63(1):29–43. Epub 2004/09/21. DOI: 10.1002/pros.20155 [PubMed: 15378522]

32. Pancrazio JJ, Viglione MP, Tabbara IA, Kim YI. Voltage-dependent ion channels in small-cell lung cancer cells. Cancer Res. 1989; 49(21):5901–6. Epub 1989/11/01. [PubMed: 2477149]
33. Johansson S, Rydqvist B, Swerup C, Heilbronn E, Arhem P. Action potentials of cultured human oat cells: whole-cell measurements with the patch-clamp technique. Acta Physiol Scand. 1989; 135(4):573–8. Epub 1989/04/01. DOI: 10.1111/j.1748-1716.1989.tb08619.x [PubMed: 2544079]
34. Blandino JK, Viglione MP, Bradley WA, Oie HK, Kim YI. Voltage-dependent sodium channels in human small-cell lung cancer cells: role in action potentials and inhibition by Lambert-Eaton syndrome IgG. J Membr Biol. 1995; 143(2):153–63. Epub 1995/01/01. [PubMed: 7731034]
35. McCann FV, Pettengill OS, Cole JJ, Russell JA, Sorenson GD. Calcium spike electrogenesis and other electrical activity in continuously cultured small cell carcinoma of the lung. Science. 1981; 212(4499):1155–7. [PubMed: 6262914]
36. Pinto JE, Viglione PN, Rothlin RP, Gomez C. Decrease of extracellular pH associated with the secretion of catecholamines induced by barium in perfused bovine adrenal medulla. Gen Pharmacol. 1993; 24(2):503–8. [PubMed: 8387059]
37. Fiske JL, Fomin VP, Brown ML, Duncan RL, Sikes RA. Voltage-sensitive ion channels and cancer. Cancer and Metastasis Reviews. 2006; 25(3):493–500. [PubMed: 17111226]
38. Benatar M, Blaes F, Johnston I, Wilson K, Vincent A, Beeson D, Lang B. Presynaptic neuronal antigens expressed by a small cell lung carcinoma cell line. Journal of neuroimmunology. 2001; 113(1):153–62. [PubMed: 11137587]
39. Dai H, Li R, Wheeler T, de Vivar AD, Frolov A, Tahir S, Agoulnik I, Thompson T, Rowley D, Ayala G. Pim-2 upregulation: Biological implications associated with disease progression and perinueral invasion in prostate cancer. The Prostate. 2005; 65(3):276–86. [PubMed: 16015593]
40. Ayala GE, Dai H, Tahir SA, Li R, Timme T, Ittmann M, Frolov A, Wheeler TM, Rowley D, Thompson TC. Stromal antiapoptotic paracrine loop in perineural invasion of prostatic carcinoma. Cancer Res. 2006; 66(10):5159–64. [PubMed: 16707439]
41. Silva J, Pinto R, Carvallho T, Coelho A, Avelino A, Dinis P, Cruz F. Mechanisms of prostate atrophy after glandular botulinum neurotoxin type a injection: an experimental study in the rat. Eur Urol. 2009; 56(1):134–40. Epub 2008/07/25. DOI: 10.1016/j.eururo.2008.07.003 [PubMed: 18649990]
42. Zhang B, Kirov S, Snoddy J. WebGestalt: an integrated system for exploring gene sets in various biological contexts. Nucleic Acids Res. 2005; 33(Web Server issue):W741–8. Epub 2005/06/28. DOI: 10.1093/nar/gki475 [PubMed: 15980575]

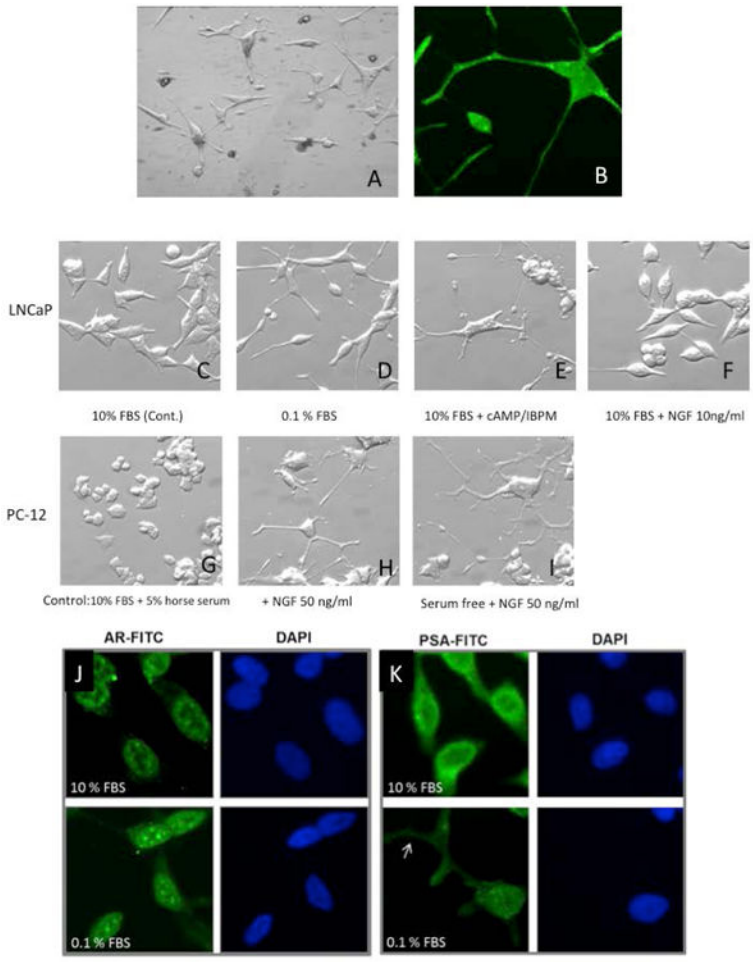

Figure 1.

[A] Morphological changes resembling neurons in LNCaP cells in vitro. LNCaP cells develop primary, secondary and tertiary branching, better seen in [B] immunostained with S-100. [C] LNCaP cells (Control day 5). [D] Cells demonstrate morphologic changes consistent with neuronal phenotype when stressed with low (0.1%) serum media or [E] Similar changes seen with cAMP [F]. These morphological changes were reversed in LNCaP cells with reintroduction of 10% serum. These morphological features are similar to those seen in PC12 cells [Controls in G] treated with nerve growth factor (NGF), an accepted model for neurons. [Seen in H and accentuated in I]. Immunohistochemistry to assess phenotypic changes of LNCaP cells under varying culture conditions. LNCaP cells (day 9) demonstrate [J] decreased expression of extranuclear AR and [K] decreased overall expression of PSA when cultured in serum deprived media, including in cellular processes (arrow), indicating dedifferentiation. DAPI nuclear staining is shown in blue. All images are 400x.

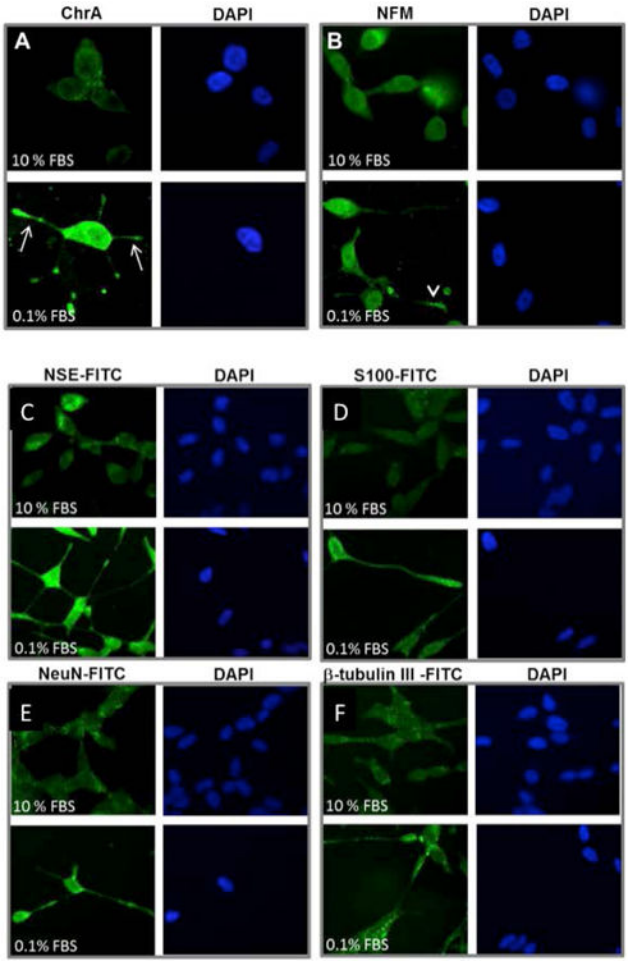

Figure 2.

LNCaP cells treated with serum starvation (day 5) express higher levels of neuroendocrine markers Chromogranin A (ChrA) [A] and Neurofilament M (NF-M) [B] compared to controls in the upper level. Marker in green (FITC) and DAPI nuclear staining is shown in blue. LNCaP cells treated with serum starvation (day 5) express higher levels of neuroendocrine markers neuron specific enolase (NSE) [C] and S-100 [D]; NeuN [E] and beta tubulin [F], compared to controls in the upper level. Marker in green (FITC) and DAPI nuclear staining is shown in blue.

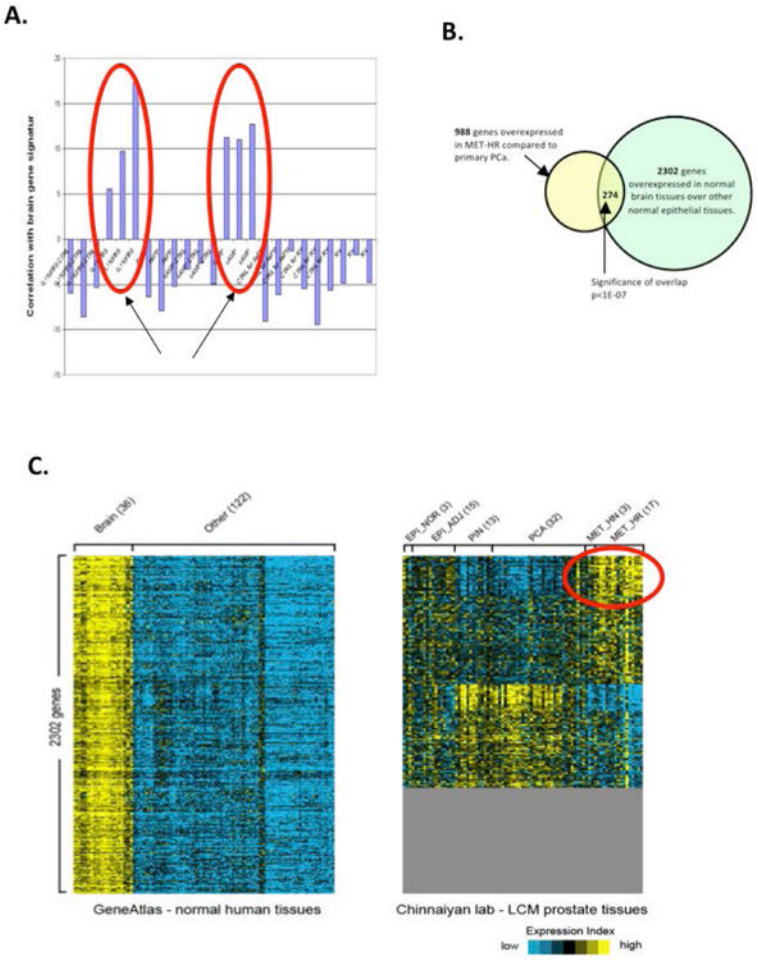

Figure 3.

A: Serum starvation (0.1%FBS) and cyclic AMP treatment of LNCaP cells groups show manifestation of the human brain signature (anything above 2 could be considered significant), but not with the transfection with S4F and ASPP2.

B: In tissue microarrays, 274 of 988 overexpressed genes in MET-HR are consistent with a “brain profile”, confirming the enrichment of the brain profile in metastatic hormone resistant prostate cancer.

C: Brain profile obtained from publically available databases in the left panel. The right panel shows prostate epithelium and cancer of different stages from left to right: normal epithelium (EPI_NOR), epithelium adjacent to cancer (EPI_ADJ), high grade PIN (PIN), prostate cancer (PCA), hormone sensitive metastatic prostate cancer (MET_HN) and hormone resistant metastatic prostate cancer (MET_HR). Note that the enrichment of genes identified in the “brain profile” is seen only in the latter.

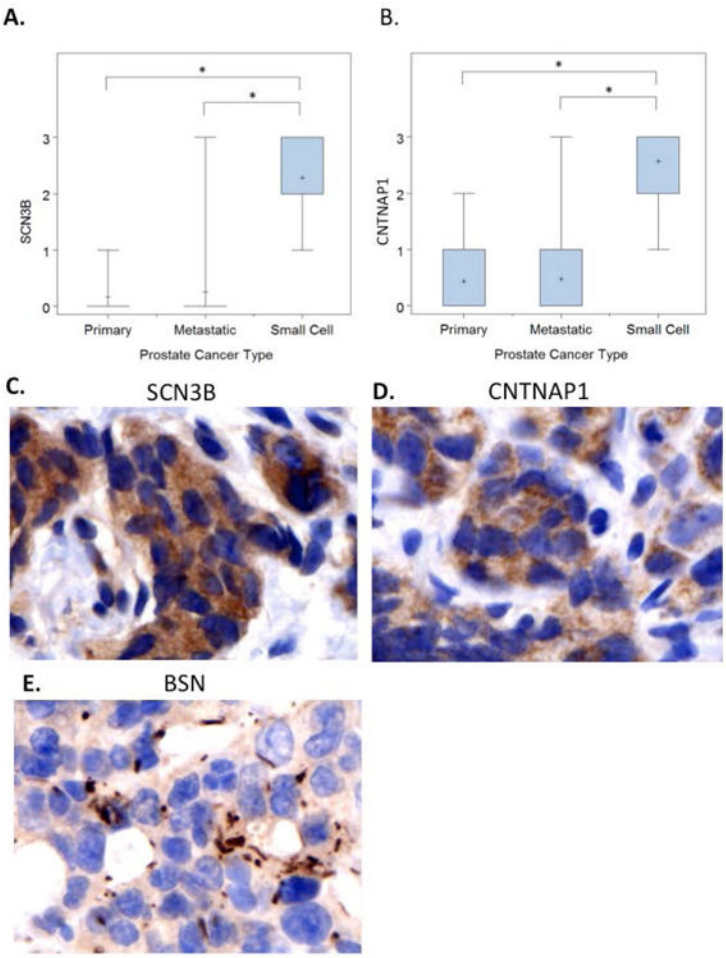

Figure 4.

A and B: Semiquantitative evaluation of immunohistochemical stains for both SCN3B and CNTNAP1 show increased levels of expression in SCC of the prostate, than primary prostate cancers or non-treated metastasis.

C and D: Microgranular cytoplasmic stain with antibodies against SCN3B and CNTNAP1, in brown (DAB: brown and hematoxylin background, 600×).

E: Membranous/cytoplasmic structures identified with antibodies against the presynaptic protein BSN (DAB: brown and hematoxylin background, 600×).

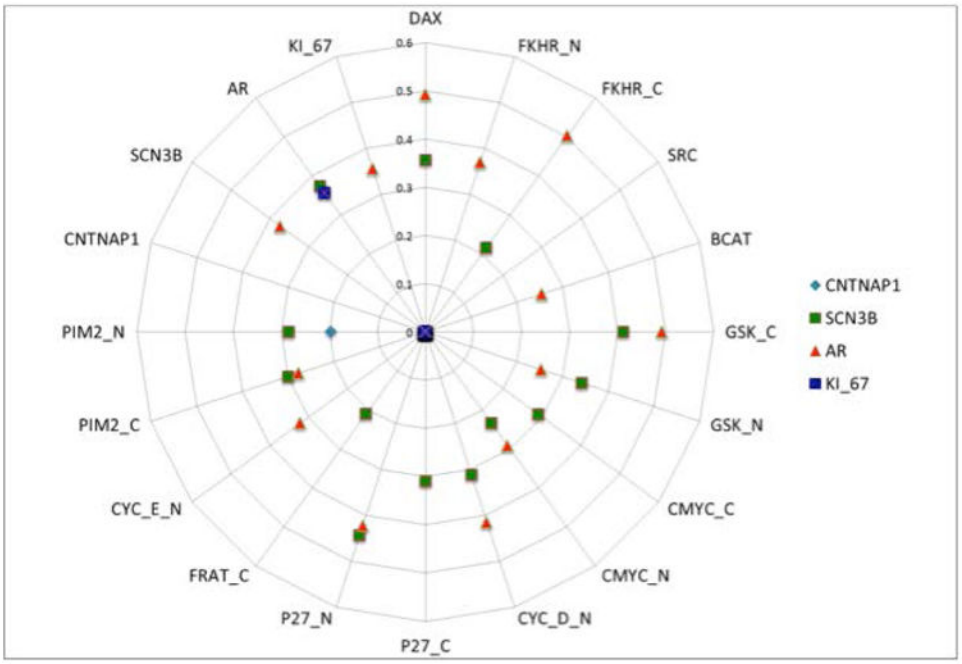

Figure 5.

Spearmen correlation coefficient analysis shows immunohistochemical co-localization of SCN3B and AR in tested MET-HN human tissue samples. A correlation between CNTNAP1 and Pim-2 was also noted.

Table 1
Up Regulated Genes in MET-HR PCa and Brain Compared *in silico*

	# Genes (of 274)	*p*-value
Biological Processes		
Anatomical structure development	74	1.84e-05
System development	70	1.86e-05
Nervous system development	54	3.85e-12
Central nervous system development	25	5.92e-06
Transmission of nerve impulse	23	2.10e-05
Synaptic transmission	21	2.61e-05
Neuron projection development	19	2.10e-05
Cell part morphogenesis	18	2.10e-05
Cell morphogenesis involved in neuron differentiation	17	2.72e-05
Neuron projection morphogenesis	17	2.72e-05
Molecular Function		
Protein binding	164	6.59e-05
Ribonucleotide binding	52	7.60e-03
Purine ribonucleotide binding	52	7.60e-03
Kinase activity	27	7.60e-03
Cytoskeletal protein binding	21	2.00e-03
Protein tyrosine kinase activity	20	7.60e-03
GTPase activity	15	1.20e-03
Protein complex binding	12	2.00e-03
Tubulin binding	7	7.60e-03
Brain-specific angiogenesis inhibitor activity	3	7.60e-03
Cellular Component		
Cytoplasm	152	3.66e-07
Cytoskeleton	40	5.00e-04
Cell traction	37	2.82e-05
Cell projection	29	2.38e-05
Synapse	25	3.83e-08
Neuron projection	22	4.85e-07
Synapse	18	2.66e-06
Axon	13	1.76e-05
Dendrite	12	2.00e-05
Synaptosome	11	1.41e-06

Table 2
Down Regulated Genes in MET-HR PCa and Brain Compared *in silico*

	# Genes (of 163)	*p*-value
Biological Processes		
Cellular component organization	46	5.90e-03
Organelle organization	30	8.80e-03
Cellular localization	28	4.80e-03
Vesicle-mediated transport	15	3.03e-02
Cellular homeostasis	14	2.43e-02
Regulation of cellular component organization	13	3.03e-02
Cellular component morphogenesis	13	3.03e-02
Microtubule-based process	12	4.80e-03
Cell morphogenesis	12	3.03e-02
Microtubule cytoskeleton organization	8	1.46e-02
Molecular Function		
Protein binding	95	4.88e-02
Protein transporter activity	6	1.95e-02
Phosphoprotein phosphatase activity	6	8.38e-02
SNARE binding	3	8.23e-02
Beta-catenin binding	3	4.88e-02
Syntaxin binding	3	4.88e-02
Transmembrane receptor protein phosphatase activity	3	1.95e-02
Transmembrane receptor protein tyrosine phosphatase activity	3	1.95e-02
Calcium-dependent protein serine/threonine phosphatase activity	2	1.95e-02
Syntaxin-1 binding	2	4.88e-02
Cellular Component		
Intracellular	124	7.00e-04
Intracellular part	123	1.00e-04
Cytoplasm	101	6.43e-07
Cytoplasmic part	66	1.40e-03
Organelle part	58	1.40e-03
Microtubule cytoskeleton	17	3.00e-04
Neuron projection	13	6.00e-04
Endosome	11	1.50e-03
Microtubule	11	1.10e-03
Centrosome	9	1.50e-03